A New Blind Adaptive Antenna Array for GNSS Interference Cancellation

Guillaume CARRIE[1], François VINCENT[1], Thierry DELOUES[2], David PIETIN[3], Alain RENARD[4]
[1]ENSICA - 1 place Emile Blouin, 31056 Toulouse Cedex 5, FRANCE
[2]ONERA/DEMR - 2 avenue Edouard Belin, BP 4025, 31055 Toulouse Cedex 4, FRANCE
[3]DGA/LRBA - 27207 Vernon, FRANCE
[4]THALES - 25 rue Jules Vedrines, 26027 Valence, FRANCE

***Abstract* - This paper introduces a new blind adaptive antenna array as a possible solution to the interference cancellation problem. This new technique is compared to three classical ones over two different sensor radiation patterns. Special attention is paid to the array compatibility with a conventional GNSS receiver. A wide radiation pattern sensor is shown to improve the positioning accuracy by maximizing the satellite constellation visibility. Finally, the new processor demonstrates its superiority in term of positioning accuracy in presence of strong interferences. However, its phase response may make it incompatible with classical GNSS receivers. Some efforts must be done to stabilize it.**

I. INTRODUCTION

Due to low SNR, GPS receivers with Fixed Radiation Pattern Antennas (FRPA) are susceptible to jamming threats. In the narrow band case, some adaptive temporal filters have been studied [1]. But in case of wideband strong interferers, a powerful technique for enhancement of GPS signal reception is the use of adaptive arrays. Several works have been carried out to study arrays hybridized with receivers [2], [3]. The solution to the interference problem which is pursued in this paper is the use of blind nullformers; that means nullformers that neither use a priori knowledge on the platform attitude nor on signals directions of arrival. This solution is particularly interesting because it requires neither modification of a conventional GNSS receiver nor connections with the platform inertial systems.

A general issue of adaptive antenna arrays is to improve the output SINR. In the particular case of GNSS systems the diversity of source directions is also of great importance in order to achieve good Geometric Dilution Of Precision (GDOP). This last point will receive most of the attention in this study.

This paper starts with an overview of classical blind nullformers. Then a new approach is introduced. Numerical simulations have been performed to compare the solutions performances. The output Signal to Noise plus Interference Ratio (SINR) and user relative positioning error are presented versus the platform attitude using real world GPS positions. The influence of single sensor radiation pattern has also been observed. Finally, attention is paid to the full compatibility with a classical GNSS receiver by observing the phase stability of the array's response.

II. DATA MODEL

Consider an array of m sensors illuminated by one useful and one jamming signals (respectively 'u' and 'j'), the output can be written:

$$\mathbf{y}(t) = \mathbf{a}_u .u(t) + \mathbf{a}_j .j(t) + \mathbf{n}(t) \quad (1)$$

where $\mathbf{n}(t)$ is a White Gaussian Noise. $\mathbf{a}_{u,j}$ denote the steering vectors of the array. Single sensor radiation patterns are included into the steering vectors.

The basis for this paper is the cascade array configuration. The complex weight vector $\mathbf{w}$ is controlled in phase and amplitude by the array processor to form the nullformer output $y_s(t)$:

$$y_s(t) = \mathbf{w}^H \mathbf{y}(t) \quad (2)$$

The auto-correlation matrix $\mathbf{R}$ of the array is the mathematical expectation E of $\mathbf{yy}^H$. All the incoming signals are assumed uncorrelated:

$$\mathbf{R} = \mathrm{E}\left(\mathbf{y}\mathbf{y}^H\right) = P_u .\mathbf{a}_u \mathbf{a}_u^H + P_j .\mathbf{a}_j \mathbf{a}_j^H + \sigma^2 .\mathbf{I} \quad (3)$$

where $P_{u,j}$ denote the powers of the incoming signals, σ^2 is the noise power and $\mathbf{I}$ is the m order identity matrix.

Due to low SNR (lower than -30dB with a 20MHz bandwidth for GPS P code signals), $\mathbf{R}$ is assumed to contain interference plus noise only.

$$\mathbf{R} \approx P_j .\mathbf{a}_j \mathbf{a}_j^H + \sigma^2 .\mathbf{I} = \mathbf{C} \quad (4)$$

II. CLASSICAL NULLFORMERS

Classically in the GNSS context, blind nullformers are designed so as to receive signals from as many satellites as possible while rejecting strong interferers. The most widely used solution consists in minimizing the array output power while trying to maintain the interference free case beampattern:

$$\min_{\mathbf{w}} \mathbf{w}^H \mathbf{R}\mathbf{w} \ / \ \mathbf{w}^H \mathbf{w}_0 = 1, \tag{5}$$

where $\mathbf{w}_0$ is the weight vector design for the desired beampattern. The solution is given by:

$$\mathbf{w} = \frac{\mathbf{R}^{-1}\mathbf{w}_0}{\mathbf{w}_0^H \mathbf{R}^{-1}\mathbf{w}_0}. \tag{6}$$

Due to their low power, this technique will not aim at canceling GNSS signals.

The most popular application of this technique, named **Power Inversion** [2] [4], is obtained with $\mathbf{w}_0 = \delta_1$, where

$$\boldsymbol{\delta}_1 = \begin{bmatrix} 1 & 0 & \cdots & 0 \end{bmatrix}^T, \tag{7}$$

and simply consists in minimizing the output power of the array while not weighting a reference sensor. Note that in the interference free case, the radiation pattern of the array is the same as the reference sensor.

To achieve better sky coverage, one can design a **Quiescent Pattern** nullformer which aims at creating an omni directional pattern in the interference free case. By least square synthesis, the desired weight vector is shown to be [5]:

$$\mathbf{w}_0 = \frac{1}{\pi^2} \boldsymbol{\Gamma}^{-1} \int_0^{\pi/2} \int_0^{2\pi} \mathbf{a}(\theta,\varphi) d\theta d\phi, \tag{8}$$

where

$$\boldsymbol{\Gamma} = \frac{1}{\pi^2} \int_0^{\pi/2} \int_0^{2\pi} \mathbf{a}(\theta,\varphi).\mathbf{a}(\theta,\varphi)^H \, d\theta d\phi \tag{9}$$

and $\mathbf{a}(\theta,\varphi)$ is the column steering vector of the array illuminated by a discrete narrow band source located at azimuth φ and elevation $(\pi/2-\theta)$ in the local reference mark of the array. $\boldsymbol{\Gamma}$ is the mathematical expectation of the array auto-correlation matrix over its visible region. Assuming no geometry mask angle, this region corresponds to the positive local elevation angles.

As no prior knowledge is assumed available on the satellites locations nor on the platform attitude, no particular Direction Of Arrival (DOA) is to be privileged. Hence, the angular probability density function (pdf) of the steering vector is taken uniform equal to $1/\pi^2$.

We can note that in the case of zero dB gain omni directional pattern sensors, if the reference sensor is the first one, the first element of any steering vector is unity and then $\mathbf{w}_0$ reduces to:

$$\mathbf{w}_0 = \boldsymbol{\Gamma}^{-1}\boldsymbol{\Gamma}(:,1) = \boldsymbol{\delta}_1. \tag{10}$$

Finally, a last technique no longer consists in a linearly constrained power minimisation: as the pdf of the GPS satellite's directions is available (a first order approximation is given in cosine of the elevation [4]), an **Optimum mean SINR** nullformer can be designed [3]. The problem consists in maximizing the mean SINR for the known spatial distribution of satellites:

$$\max_{\mathbf{w}} \frac{\mathbf{w}^H \boldsymbol{\Gamma}_{mean} \mathbf{w}}{\mathbf{w}^H \mathbf{R}\mathbf{w}}, \tag{11}$$

where $\boldsymbol{\Gamma}_{mean}$ is the mean autocorrelation matrix of the array related to the known spatial distribution of satellites:

$$\boldsymbol{\Gamma}_{mean} = \frac{1}{2\pi} \int_0^{\pi/2} \int_0^{2\pi} \mathbf{a}(\theta,\varphi).\mathbf{a}(\theta,\varphi)^H \sin(\theta).d\theta d\phi. \tag{12}$$

The optimum weight vector is shown to be [5] the principal eigenvector of $\mathbf{R}^{-1}\boldsymbol{\Gamma}$.

III. A NEW APPROACH

A drawback of the last nullformer is the requirement for knowledge of the platform attitude to determine the upward direction, which is not supposed available in the case of blind processor.

As an alternative, we propose the **Maximum Aperture** nullformer. As the platform attitude is unknown, we use a uniform probability density function to evaluate mean spatial properties of the array. Then, we define the array angular aperture as the ratio:

$$\tilde{\theta}^2 = \frac{\int_0^{\pi/2} \int_0^{2\pi} G(\theta,\varphi)\theta^2 d\theta d\phi}{\int_0^{\pi/2} \int_0^{2\pi} G(\theta,\varphi) d\theta d\phi}, \tag{13}$$

where $G(\theta,\varphi)$ is the array radiation pattern:

$$G(\theta,\varphi) = \left| \mathbf{w}^H.\mathbf{a}(\theta,\varphi) \right|^2. \tag{14}$$

Hence, the array angular aperture reduces to:

$$\tilde{\theta}^2 = \frac{\mathbf{w}^H \boldsymbol{\Gamma}_{\theta^2} \mathbf{w}}{\mathbf{w}^H \boldsymbol{\Gamma} \mathbf{w}}, \tag{15}$$

where $\boldsymbol{\Gamma}$ is defined such as in (8) and:

$$\boldsymbol{\Gamma}_{\theta^2} = \frac{1}{\pi^2} \int_0^{\pi/2} \int_0^{2\pi} \mathbf{a}(\theta,\varphi) \mathbf{a}(\theta,\varphi)^H \theta^2 d\theta d\phi. \tag{16}$$

We can note that $\boldsymbol{\Gamma}$ and $\boldsymbol{\Gamma}_{\theta^2}$ are only dependant on the array geometry and single sensor radiation pattern.

Canceling the interferences while maximizing the array aperture would be of interest in order to emphasis with good GDOP. In order to satisfy as well as possible the two aims at cost of only one degree of freedom, we chose to maximize the product of the array aperture with the mean SINR:

$$\max_{\mathbf{w}} \left(\frac{\mathbf{w}^H \boldsymbol{\Gamma}_{\theta^2} \mathbf{w}}{\mathbf{w}^H \boldsymbol{\Gamma} \mathbf{w}} \times \frac{\mathbf{w}^H \boldsymbol{\Gamma} \mathbf{w}}{\mathbf{w}^H \mathbf{R} \mathbf{w}} \right). \tag{17}$$

Then, the weight vector solution is the principal eigenvector of $\mathbf{R}^{-1}\boldsymbol{\Gamma}_{\theta^2}$.

IV. Numerical Simulations

We now wish to evaluate the performances of these four processors. Simulations have been performed with a seven elements hexagonal array structure. The inter element spacing is chosen to be half wavelength (represented by solid lines on Fig. 1) so that mutual coupling is minimized and grating lobes are prevented.

Single sensor radiation pattern also influences the performances. Thus, a wideband array simulator has been developed; including the radiation patterns of two real sensors (see Fig. 2). The first one is described in [6], the second one has been extrapolated from data found in [7].

Several simulations have been run involving real GPS orbits sampled at one point per half hour. Then results have been averaged over a 24 hours period in order to provide a global sight of the GPS constellation. The results are presented as functions of the platform pitching angle. The pitching information is not fed into the Optimum SINR technique.

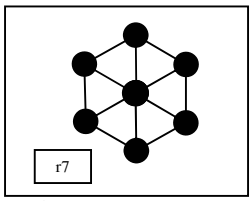

Fig. 1. Array geometry.

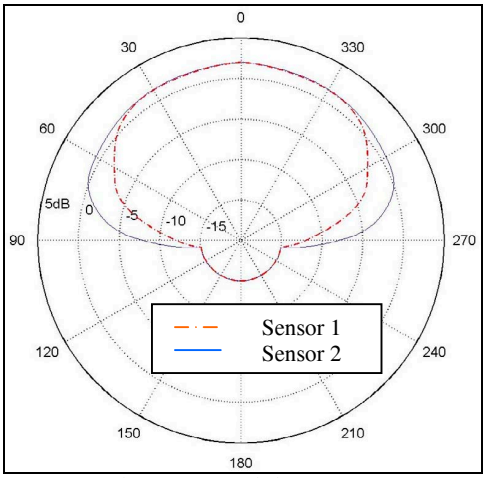

Fig. 2. Sensor radiation patterns.

As a performance criterion, we use the standard deviation of the user positioning error, approximated by [2]:

$$\sigma_{pos} = \sqrt{Tr\left(\left(\mathbf{A}^T \mathbf{D} \mathbf{A}\right)^{-1}\right)}, \tag{18}$$

where $\mathbf{A}$ is the Geometry matrix, $\mathbf{D}$ should be the inverse diagonal matrix of User Equivalent Range Error (UERE) by satellite and is approximated by the diagonal matrix of SINR by satellite. *Tr* denotes the trace of a square matrix. When interferences are introduced, we evaluate (18) using only the useful signals that exceed a signal to jammer power ratio threshold of - 41 dB. In that case, the mean number of satellites that exceed this threshold is also presented.

The standard deviation of the user positioning error presented is normalized by the one reached by the sensor 1 (see Fig. 2) alone for a zero pitching angle and in white noise context only.

In white noise context only, for the two single radiation patterns simulated, the Power Inversion technique exhibits the best positioning accuracy while some techniques produce better SINR. This is illustrated on Fig. 3. Indeed, the other techniques constrain the array radiation pattern to compensate for the weak gain at low elevations where GNSS satellites are mostly located. This makes the gain drop at local zenith of the array, resulting in a degraded GDOP (see Table I).

We can also observe that the higher the pitching, the lower the accuracy. This is due to degradation of the constellation visibility. Finally, the wider the single sensor radiation pattern, the more accurate the positioning.

These two last conclusions remain true when interferences are introduced. This is illustrated on the following Fig. 4 where two strong interferers are respectively located at elevations 10° and 30°, azimuths 30° and 130° with Jammer to Noise power Ratio (JNR) equal to 20 dB and 40 dB.

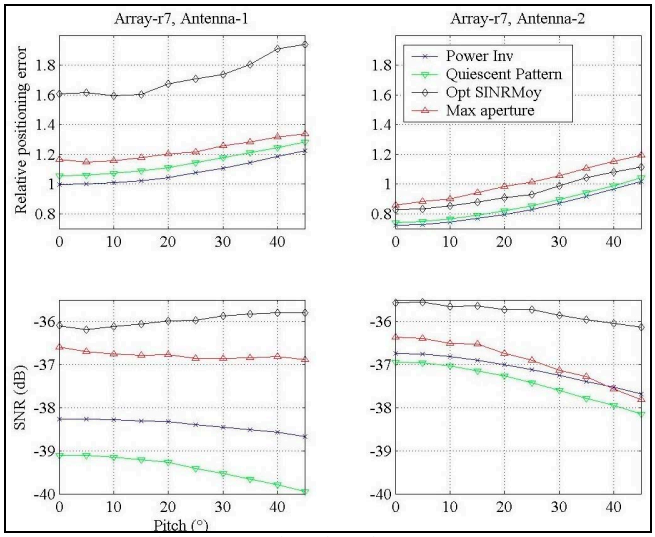

Fig. 3. Array r7 in white noise context only.

In that context, we can observe a difference of behavior between the two classes of techniques: the linearly constrained power minimization techniques (class 1) and the ratio maximization ones (class 2). Especially, with sensor 2 (see Fig.2) the difference between nullformers of a same class is reduced and there remain nearly no difference between the Power Inversion and the Quiescent Pattern nullformers.

Due to its widening effect, the maximum aperture technique exhibits good performances compared to other nullformers, especially with the sensor 1 whose aperture is relatively narrow. When applied to the sensor 2, the four nullformers provide different average SINR, however they provide the same positioning error until the pitching angle reaches 30°. For higher pitching angles, despite the mean SINR of our new nullformer remains low, its wide aperture allows more satellites to be locked by a classical GNSS receiver, resulting in the best positioning accuracy (see Fig.4).

Finally, the Maximum aperture nullformer produces a good accuracy even if it does not provide the best SINR. Especially for high pitching angles where the performances of the other nullformers can be more severely degraded: its large aperture makes it less sensitive to the platform attitude.

TABLE I
NULLFORMERS PARAMETERS IN ASYMPTOTIC WHITE NOISE WITH SENSOR 2

Nullformer	3dB beamwidth (steradian)	$\tilde{\theta}$ (°)	White noise gain at zenith (dB)	White noise maximum gain (dB)
Power Inversion	4.64	44.3	2	2
Quiescent Pattern	5.23	48.6	-0.3	0.9
Optimum mean SINR	1.04	43.7	-289	7.6
Maximum aperture	0.66	59.5	-303	6.7

V. PHASE STABILITY

The weighted array must not deteriorate the desired signal phase. Indeed, the range measurements in the receiver are based upon carrier and code tracking loops. Despite the desired signal power exceeds the required threshold; the carrier loop can break because of phase jumps.

This last section explores the phase jumps of the array's responses due to the weight vectors calculation. The basis assumption for this calculus is as follows: the array auto-correlation matrix is estimated using a succession of snapshots. The weight vectors are then calculated as described in sections II and III. Then they are applied to the snapshots used to estimate the auto correlation matrix. There is no overlap between two successions of snapshots.

We first noted that the array phase response can widely vary for angles close from the interferers' locations. This does not affect the array performances because the desired signal power does generally not exceed the tracking threshold in that region.

We also noted that the behaviors are very similar for the nullformers of the same class but quite different from class 1 to class 2. This difference is illustrated on Fig. 5 where we present the mean and standard deviation of phase jumps over 100 simulations of the same scenario. The simulation involves the two previously presented jammers and a GNSS satellite located at elevation 10° and azimuth 80°. The results are presented as a function of the number of snapshots used to estimate the auto-correlation matrix of the array; a 3 dB diagonal loading is applied.

In such a situation, the satellite is far enough from the jammers so that its power enables a classical receiver to track it. However the instability of the array phase response may unlock the tracking loop.

As a conclusion of this section, we observed that nullformers of class 2 have an instable phase response even far from the interferences locations. Efforts must be made to stabilize it in order to make these array processors compatibles with classical GNSS receivers. In that way, the use of symmetric arrays with conjugate symmetric weightings may produce interesting solutions by forcing a null imaginary part of the array response.

CONCLUSIONS

Four processors have been simulated in several configurations with two different sensor radiation patterns.

A first general conclusion is that the higher the pitching, the lower the positioning error. This is due to degradation of the constellation visibility.

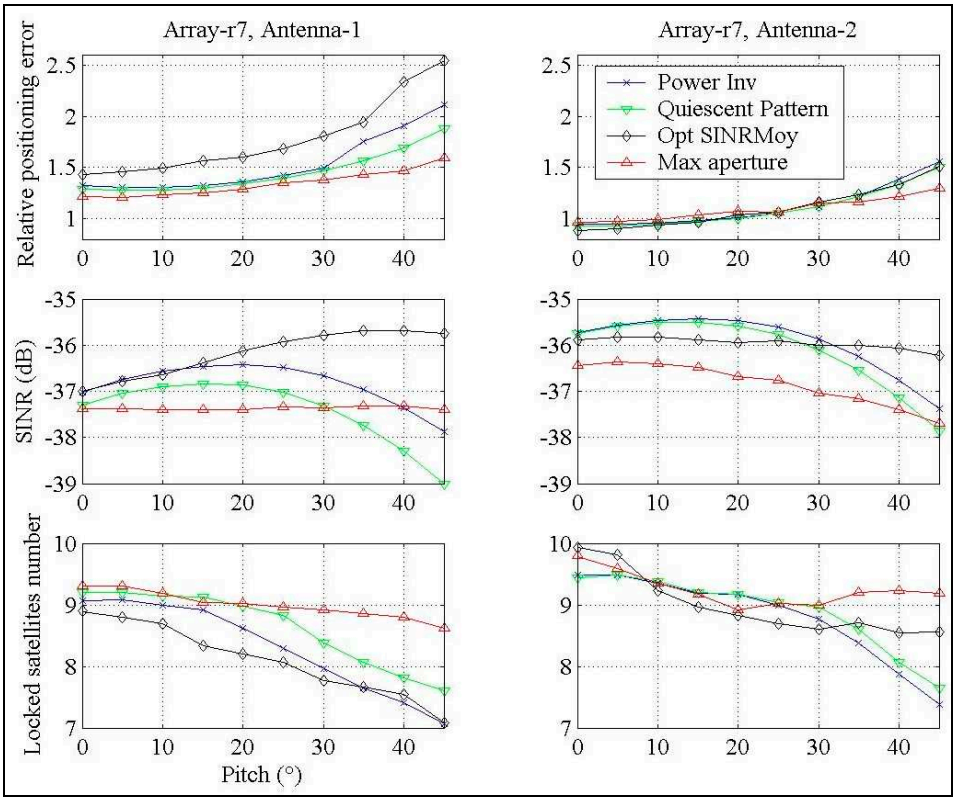

Fig. 4. Array r7 in presence of two strong interferers.

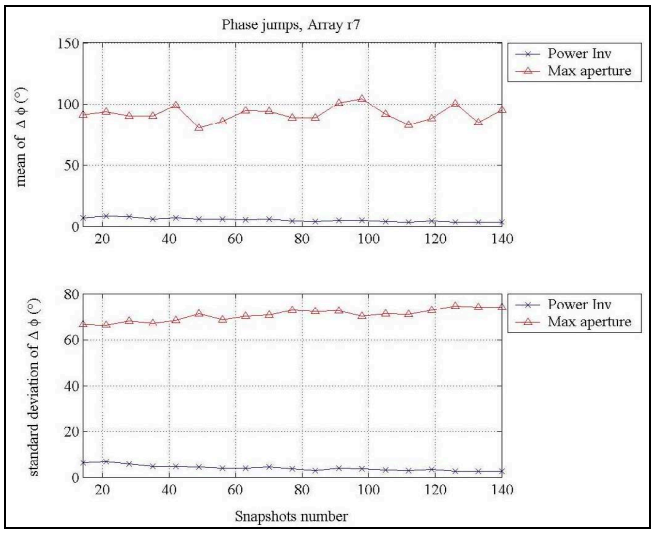

Fig. 5. Phase jumps 'far' from the interferers with a 3 dB Diagonal Loading.

The single sensor radiation pattern is also of great importance: the wider the single sensor radiation pattern, the more accurate the positioning. We can also note that with sensor 2, the difference between nullformers of a same class is reduced.

Finally, it has been found that in terms of positioning accuracy, the Power Inversion outperforms all other techniques for every configuration in the white noise environment; while the Maximum Aperture nullformer produces most often the best accuracy in presence of strong interferers even if it does not provide the best SINR. However, because of the instability of its phase response, its compatibility with a classical GNSS receiver is not guarantied. Some efforts must be performed in order to stabilize it.

REFERENCES

[1] R. Jr. Landry, D. Lekaïm, P. Mouyon, "Narrow Band Signal Rejection in AWGN by Wavelet Coefficients Thresholding", PIERS 97, Boston, July 1997.

[2] D-J. Moelker, Dr. Y. Bar-Ness, "An Optimal Array Processor for GPS Interference Cancellation", IEEE 1996.

[3] R.L. Fante, J.J. Vaccaro, "Wideband Cancellation of Interference in a GPS Receive Array", IEEE TRANSACTIONS ON AEROSPACE AND ELECTRIC SYSTEMS, vol. 36, n° 2, april 2000.

[4] D-J. Moelker, E. Van der Pol, Dr. Y. Bar-Ness, "Adaptive Antenna Arrays for Interference Cancellation in GPS and Glonass Receivers", IEEE 1996.

[5] H. L. Van Trees, "Optimum Array Processing, Part IV of Detection, Estimation, and Modulation Theory", WILEY-INTERSCIENCE 2002.

[6] H. Ly, P. Eyring, E. Traum, H-W. Tseng, K. Stolk, et al., "Design, Simulation, and Testing of a Miniaturized Dual-Frequency (L1/L2) Antenna Array", Proceedings of ION GPS 2002. Portland Oregon September 2002.

[7] Z-B. Lin, R. Castillo, J. J-Q. Lin, S. Robin, "Miniaturisation of L1/L2 Anti-jam GPS Antenna Array", ION GPS 2002, 24-27 September 2002, Portland, OR.